Quantifying individual differences in brain morphometry underlying symptom severity in Autism Spectrum Disorders

Emmanuel Peng Kiat Pua[1,2], Gareth Ball[2], Chris Adamson[2], Stephen Bowden[1,4], and Marc L Seal[2,3]

Author Affiliations

[1] Melbourne School of Psychological Sciences, University of Melbourne, Australia

[2] Developmental Imaging, Murdoch Children's Research Institute, Australia

[3] Department of Paediatrics, University of Melbourne, Australia

[4] St. Vincent's Hospital, Melbourne, Australia

Corresponding Author

Emmanuel Pua

Developmental Imaging, Murdoch Children's Research Institute

50 Flemington Rd, The Royal Children's Hospital, Parkville, VIC 3052, Melbourne, Australia

+61 (03) 99366420

emmanuel.pua@mcri.edu.au

Abstract

Neurobiological mechanisms underlying heterogeneous neurodevelopmental disorders such as autism spectrum disorders (ASD) are still poorly defined. Despite extensive efforts to delineate the link between brain morphometry and ASD symptomatology, majority of findings are not reproducible due to high levels of individual variance in phenotypic expression. To investigate if individual differences in brain morphometry are important features in ASD symptom severity, we implemented a novel subject-level, distance-based method using subject-specific attributes of cases and controls. In a large multi-cohort sample, each subject with ASD (n=100; n=84 males; mean age: 11.43 years; mean IQ: 110.58) was strictly matched to a control participant (n=100; n=84 males; mean age: 11.43 years; mean IQ: 110.70) to ensure homogeneity on age, IQ, sex and image acquisition site. The intrapair Euclidean distance of MRI brain morphometry and symptom severity measures were entered into a regularized machine learning pipeline for feature selection modelling, with rigorous out-of-sample validation and bootstrapping for permutation testing. Subject-specific cortical thickness (19 features; p=0.01, n=5000 permutations) and surface area (10 features; p=0.006, n=5000 permutations) features significantly account for individual variation in ASD symptom severity. The association between unique variation in brain features and symptom severity remained robust across subjects and were replicated in validation samples. Identified cortical regions strongly implicate the involvement of key hubs of the salience and default mode networks as neuroanatomical features of social impairment in ASD. The new findings highlight the importance of subject-level markers in ASD, and offers important step forward in understanding the neurobiology of heterogeneous disorders.

Introduction

Definitive aetiologies in neurodevelopmental disorders such as autism spectrum disorders (ASD) remain poorly defined due to significant heterogeneity within and between individuals[1]. ASD are a group of neurodevelopmental conditions characterized by impairments in social communication and restricted and repetitive behaviours. Magnetic Resonance Imaging (MRI) offers an in vivo method to assay neurobiological abnormalities, and has produced promising findings of brain dysfunction in ASD[2]. However, group differences in brain structure or function in ASD are still frequently misidentified because of the high levels of variability between and within individuals, resulting in poor reliability and reproducibility of findings [3].

In addition to the large phenotypic variation in individuals with ASD, neuroimaging studies are confounded by a number of methodological factors related to differences in image acquisition sites, anatomical sex, IQ, as well as age-dependent perturbations of neurodevelopment [4]. Alterations in brain structure and function in ASD relative to neurotypical peers demonstrate a continuous shift throughout the lifespan, and the nature or trajectory of these abnormalities are also likely differ between individuals with the condition [5]. Consequently, efforts to identify consistent differences in the brain in individuals with ASD have thus remained largely unsuccessful, and there is a need for predictive brain-based biomarkers that are sensitive to heterogeneity in the neurobiology and symptom expression of ASD [6]

Emerging work suggests that individually specific variation in brain architecture may be a critical factor underlying idiosyncrasies in ASD symptom characteristics [7,8]. Conventional neuroimaging investigations have been of limited yield in ASD research, as such approaches typically rely on group-averaged between-group effects and do not

allow inferences on individual subjects. High-dimensional neuroimaging data with a large number of, often co-linear, features relative to small sample size pose further problems with increased risk of false positives. To overcome these roadblocks, analysis techniques must sufficiently account for these issues associated with large-scale neuroimaging data as well as subject-level predictions [9,10].

Drawing from multi-disciplinary methodologies in ecology and twin modelling [11], we developed a novel subject-level, distance-based method to test the hypothesis that neuroanatomical differences between subjects can explain individual differences in symptom severity. Using this approach on carefully matched case-control pairs, we compared s*ubject-specific* differences in brain structural morphometry on MRI to differences in individual symptom severity. Importantly, our approach implements well-validated and sophisticated machine learning and feature reduction techniques to reduce the likelihood of false positives, and to ensure the reproducibility of analyses results.

Methods

Participants

Data was obtained from the Autism Brain Imaging Database Exchange (ABIDE-II) cohort across 17 independent imaging sites [12]. Protocols specific to each imaging site for diagnosis, behavioural and cognitive assessment, and Magnetic Resonance Imaging (MRI) acquisition are publicly available[1]. The Social Responsiveness Scale (SRS-2) was used as a phenotype measure of ASD symptom severity. The instrument is commonly used for both screening and as a tool to aid clinical diagnosis. The SRS has been established to be a reliable and valid quantitative measure of ASD traits, demonstrating convergent validity with the gold standard Autism Diagnostic Observation Schedule and Autism Diagnostic Interview, and is able to discriminate ASD from other psychopathologies [13,14].

Based on the multivariate genetic matching method of Ho et al. 2011; [15], each ASD case was individually matched to the nearest control participant in age and IQ, restricted to a maximum distance of 0.25 standard deviations for each variable within each pair. For categorical variables, exact matching criteria were set for participant sex and image acquisition site. The genetic search algorithm [16] aims to achieve optimal balance after matching by finding a set of weights for each covariate of interest. Matching balance was evaluated by univariate and paired t-tests for dichotomous variables and the Kolmogrov-Smirnov test for continuous or multinomial variables. The process selected n=100 individuals with ASD to 100 controls eligible for inclusion (see Table 1).

[1] http://fcon_1000.projects.nitrc.org/indi/abide/

Image processing

Pre-processing and analysis of T1-weighted (MRI) was performed using FreeSurfer (v 6.0.0; http://surfer.nmr.mgh.harvard.edu/) for all ABIDE subjects. Briefly, the FreeSurfer cortical surface reconstruction pipeline performs the following steps in sequence: non-uniform intensity correction, skull stripping, segmentation into tissue type and subcortical grey matter structures, cortical surface extraction and parcellation. Visual inspection for movement artefacts were conducted for every subject to ensure data quality control. Manual editing was performed on the white matter mask images to avoid false-positive errors in estimated surfaces. Cortical morphometric statistics based on the Desikan–Killiany–Tourville (DKT) brain anatomical atlas were used to estimate cortical thickness (mm) and surface area measurements (mm^2) for each brain region. An advantage of the DKT atlas is that labelling is performed on a per-subject basis rather than the projection of a single parcellation onto every cortex, and is well-suited for the present subject-level analyses.

Subject-level distance-based analysis

Within-pair Euclidean distances were computed for every matched pair on clinical and demographic continuous variables of interest and cortical thickness measures. Age and intracranial volume normalization was used to obtain mean standardized residuals to adjust for age and head size disparity. By measuring the difference between matched brains at the level of individual subjects, we can examine brain-behaviour associations underlying variation in symptom severity, while increasing homogeneity by directly controlling for key neurodevelopmental confounds. Figure 1 provides a summary of the analysis pipeline. Regularized regression with elastic net penalization [17] was used to test the hypothesis that selected case-control differences in cortical morphometry were

associated with variation in symptom severity (α =0.5, λ=100, *k*-fold cross-validation=10, *n* iterations =1000). In machine learning, we aim to use data to train a model to make accurate predictions on new, unseen or held-out datasets. Elastic net is an embedded technique that combines machine learning and feature reduction functions by implementing a regularization framework to obtain a reduced subset of selected features. Elastic net has been previously applied in machine learning for neuroimaging in Alzheimer's disease classification and treatment outcome predictions in ADHD cohorts [10]. In regularized regression, λ is a parameter controlling for the strength of regularization. The higher the value of λ, the more likely coefficients will be estimated towards zero with an increased penalty. α is the mixing parameter ($0< \alpha<1$) and determines the relative quantities of L_2 norm penalized regression (ridge regression) and L_1 norm penalized regression (LASSO regularized penalization). Elastic net is an approach that combines both the L_1 and L_2 penalties of the LASSO and ridge methods.

A subset of the matched-pairs sample (33%) was held out as an out-of-sample test set independent of the subject data; that is these data were not used in the cross-validation steps (training set), and only examined as an independent validation of the model (test set). The remaining data was used as a training set to obtain optimal model weights for selected features. In the training set, we employed a strict k-fold cross-validation loop (10 folds, 1000 iterations) to train the model to predict differences in symptom severity between matched cases and controls in the out-of-sample test set. The model was trained within a k-fold cross-validation loop (k=10). The training set is first randomly partitioned into *k* subsamples of equal size. For each fold, one subsample is withheld for internal validation to test the model trained on *k-1* subsamples. Each of the *k*

subsamples were used as the validation set once per fold. Results from each fold were averaged to obtain a single estimation. Due to intrinsic randomness of model building, estimated coefficients may vary after each run. To account for stochastic error and to ensure robustness of estimates, the process was repeated for n=1000 iterations, and the averaged coefficient weights used to generate predictions in the out-of-sample test set.

Model goodness-of-fit was assessed by constructing a null distribution of symptom severity outcome. To generate a null distribution, the symptom severity (difference) variable was randomized across every sample observation of cortical thickness or surface area features using 5,000 permutations. For each iteration, model parameters were obtained using the same machine learning pipeline with regularized regression with elastic net penalty. The *p*-value of the initial model fit in the out-of-sample test set was computed as the proportion of iterations in the null distribution with model performance exceeding that of the initial model fit. Application and validation of recommended best practice for the regularized regression protocol are detailed elsewhere [18,19]. The entire procedure was repeated for cortical thickness and surface area measures. Final model weights were obtained by fitting selected features on the entire dataset to allow independent model testing. To validate our approach against group-level prediction methods, we repeated the entire machine learning pipeline on the same matched ASD cohort but at the group-level without within-pair distance computations, adjusted for age, sex, site, IQ and intracranial volume effects.

Analyses were performed in the *R* environment [20] using the *MatchIt* and *boot* wrapper tools [18,21,22]. Visualizations were generated with in-house MATLAB scripts.

Results

Using regularised linear regression to predict differences in symptom severity from differences in MRI features (Figure 2), we applied an elastic net penalty to achieve a sparse solution and select important features from the full imaging dataset. After training, the model significantly predicted differences in symptom severity between cases and controls in the out-of-sample dataset (R^2=0.153; p=0.01, 5000 permutations). Based on 1000 iterations of the training loop, nineteen cortical thickness features were retained as predictors of individual differences in symptom severity (Figure 3A; Supplementary Table 1).

The above procedure was repeated for cortical surface area measurements to predict differences in symptom severity. Ten surface area features were selected in the training dataset, with a favourable out-of-sample model fit (R^2=0.18, p=0.006; Figure 3B; Supplementary Table 2). Mean coefficient weights for the selected model features for both cortical thickness and surface area data are shown in Supplementary Figure 1.

Our approach was validated against conventional methods of group-level prediction less robust to heterogeneity across individuals. As expected, without accounting for subject-level within-pair differences, regression model training to predict symptom severity based on group-level MRI features achieved a poor fit in out-of-sample validation tests (Cortical thickness model fit: R^2= 0.0000434; surface area model fit: R^2=0.0158) by comparison. Overall, the results indicate that subject-level modelling significantly outperforms group-difference methods of symptom severity prediction in a heterogeneous disorder such as ASD. Comparisons of model fit performance for both approaches are shown in Supplementary Figure 2 and Supplementary Table 3.

Discussion

By implementing a strict matching procedure combined with subject-level distance-based prediction of variation in ASD symptom severity, we demonstrate that individual-specific differences in cortical morphology are associated with subject-level variation in ASD symptom severity. Key features implicate abnormal morphometry of frontal and temporal-parietal cortices, fusiform gyri, anterior and posterior cingulate regions and the insula. Features with the strongest coefficient weights were the right inferior temporal gyrus thickness and the left insula area.

The identified cortical regions constitute hub regions of the salience network and default mode network (DMN) that have been increasingly suspect to be aberrant in ASD [23]. The salience network (SN) primarily anchored to the anterior insular and dorsal anterior cingulate cortex contributes to cognitive and affective processes such as social behaviour and communication, and the integration of sensory, emotional and cognitive information [24]. The DMN comprising the posterior cingulate, medial prefrontal and parietal cortices typically demonstrates reduced activity on task initiation, and functions to support self-referential and introspective states and social cognition [25]. Altered function of the salience network and DMN are highly consistent with ASD symptomatology, and emerging evidence suggests that specific features of cortical regions comprising these networks may discriminate ASD from neurotypical development [2].

Regions of the frontal, temporal, fusiform and insular cortices were previously reported to be important classification features in ASD, but inferences have been limited as findings were inconsistent due to high variability in symptom severity, age and IQ across heterogeneous ASD subgroups. Classification accuracy became poorer as

subgroup differences along these variables increased, but was significantly improved by matching on subject demographics [26]. Present findings identified similar cortical features, and support the hypothesis that homogeneity between subjects can reduce noise and improve precision in ASD investigations. By modelling individual variability, patterns of abnormalities that are stable across cortical regions and subjects may emerge or become more distinct (Figure 2). To qualify as potential candidate markers in the neurobiology of ASD, it is essential that such features demonstrate significant associations with ASD symptomatology based on rigorous analysis and validation [27]. Here we go further to demonstrate that individual variation in identified cortical regions also explain differences in symptom severity at the level of the individual (Figure 3).

Importantly, a dimensional approach as such offers a more precise quantification of sub-threshold ASD traits in individuals do not meet the criteria for clinical diagnosis, otherwise known as the broader autism phenotype [28]. Investigating group differences in ASD by comparing group-averaged variables collapsed within patient and control groups are likely to obscure important subject-specific effects. For example, a broader phenotype individual in the control group may display a high degree of similarity in symptom severity to an individual with a milder presentation of ASD [29]. This pattern is observed in the current sample with overlapping symptom severity scores ranges between cases and controls. Even when matched at the group level on confounding variables, our results suggest that group-level differences are not as useful in predicting symptom severity compared to the individual distance model, at least in ASD cohorts. As we have shown, individual variability in brain morphometry and symptom severity can be identified with a subject-level distance-based approach, while also accounting for individual differences in neurodevelopment based on matching of confounds at the

individual level (rather than at the group-level) to ensure homogeneity between matched subjects. Such an approach allows for improved characterization of the heterogeneous nature of ASD that respects the continuous spectrum of symptom severity in the population.

Findings suggest that as neuroanatomy diverges between ASD and control subjects, differences in symptom severity increase. Conversely, negative coefficient weights reflect an increase in symptom severity as regional cortical features becomes less different between ASD and controls. While this may appear counterintuitive, longitudinal investigations suggest that the expected linear decline in cortical regions seen in typical development may be absent in ASD [30]. The result is an intersection of atypical cortical developmental trajectories in ASD with that of typically developing peers. At such time-points in development, group differences in abnormally developing cortical regions in ASD would fail to be observed cross-sectionally, despite a concomitant difference in symptom severity. This phenomenon may likely explain the high frequency of inconsistent findings in ASD as most studies do not adequately consider differences at the individual level.

Together these findings suggest that subject-level variation in brain properties are potentially important markers of ASD symptom severity. The present study is limited to cortical thickness and surface area features, and other properties of brain structure and function may account for larger proportions of variance in symptom severity. Complex neurodevelopment conditions such as ASD likely stem from perturbations of anatomically distributed and interconnected neural systems [31]. As brain structural connectivity constrains the development of functional networks across the lifespan, validation across different imaging modalities will be necessary to elucidate distinct

neurobiological mechanisms, such as network analysis of white matter microstructure and functional connectivity [32]. Based on the robustness and reliability of present results, cortical hubs of the salience and DMN networks are likely to be strong candidates as key neuroanatomical markers of ASD symptomatology. We strongly encourage continued multimodal subject-level distance-based investigations to test this hypothesis for ASD in large multi-site cohorts. Individual variability in heterogeneous populations such ASD should be carefully treated, rather than discarded as noise.

Conclusion

The robustness and generalizability of present findings is important progress in the search for neural correlates of heterogeneous disorders such as ASD, and offers a promising insight into the neurobiology of ASD symptomatology. Given that the endeavour is frequently hindered by problems with inconsistent replication due to inter- and intra-individual heterogeneity, investigations of heterogeneous populations such as ASD must necessarily demonstrate generalization beyond in-sample modelling as we have shown. Accounting for individual differences at the subject level allows for the reliable identification of neural correlates associated with variation in symptom severity to quantify individual variation in ASD or the broader autism phenotype. Reliable and valid evidence of subject-specific alterations in brain structure and function based on such approaches will be necessary to advance current knowledge about the aetiology of ASD, with potential applications to aid management or personalized intervention strategies for each unique patient at the individual level.

Acknowledgements

Data analysis and interpretation was conducted within the Developmental Imaging research group, Murdoch Children's Research Institute and the Children's MRI Centre, Royal Children's Hospital, Melbourne, Victoria. All procedures were conducted in accordance with the Declaration of Helsinki, and approved by The Royal Children's Hospital Human Research Ethics Committee.

The research was supported by the Murdoch Children's Research Institute, The Royal Children's Hospital, Department of Paediatrics The University of Melbourne and the Victorian Government's Operational Infrastructure Support Program. The project was generously supported by RCH1000, a unique arm of The Royal Children's Hospital Foundation devoted to raising funds for research at The Royal Children's Hospital.

Author contributions

EP designed the study, performed data analysis and visualizations and prepared the manuscript. GB contributed to the study design and manuscript preparation. CA contributed to data analysis and visualizations. SB and MS supervised the study and contributed to manuscript preparation.

Competing Financial Interests

The authors declare no potential conflicts of interest with respect to the research, authorship, and/or publication of this article.

References

1. Hahamy A, Behrmann M, Malach R. The idiosyncratic brain: Distortion of spontaneous connectivity patterns in autism spectrum disorder. *Nature Neuroscience.* 2015;18(2):302-309.
2. Uddin LQ, Dajani DR, Voorhies W, Bednarz H, Kana RK. Progress and roadblocks in the search for brain-based biomarkers of autism and attention-deficit/hyperactivity disorder. *Translational Psychiatry.* 2017;7(8):e1218.
3. Ecker C. The neuroanatomy of autism spectrum disorder: An overview of structural neuroimaging findings and their translatability to the clinical setting. *Autism : the international journal of research and practice.* 2017;21(1):18-28.
4. Pua EPK, Bowden SC, Seal ML. Autism spectrum disorders: Neuroimaging findings from systematic reviews. *Research in Autism Spectrum Disorders.* 2017;34:28-33.
5. Lange N, Travers BG, Bigler ED, et al. Longitudinal volumetric brain changes in autism spectrum disorder ages 6-35 years. *Autism Research.* 2015;8(1):82-93.
6. Jack A, Pelphrey KA. Annual Research Review: Understudied populations within the autism spectrum - current trends and future directions in neuroimaging research. *Journal of Child Psychology and Psychiatry.* 2017.
7. Chen H, Nomi JS, Uddin LQ, Duan X, Chen H. Intrinsic functional connectivity variance and state-specific under-connectivity in autism. *Human Brain Mapping.* 2017.
8. Dickie EW, Ameis SH, Viviano JD, et al. Personalized intrinsic network topography mapping and functional connectivity deficits in Autism Spectrum Disorder. *Biological psychiatry.* 2017.
9. Bzdok D, Yeo BTT. Inference in the age of big data: Future perspectives on neuroscience. *NeuroImage.* 2017.
10. Mwangi B, Tian TS, Soares JC. A review of feature reduction techniques in neuroimaging. *Neuroinformatics.* 2014;12(2):229-244.
11. Carlin JB, Gurrin LC, Sterne JA, Morley R, Dwyer T. Regression models for twin studies: a critical review. *International journal of epidemiology.* 2005;34(5):1089-1099.
12. Di Martino A, Yan C-G, Li Q, et al. The autism brain imaging data exchange: towards a large-scale evaluation of the intrinsic brain architecture in autism. *Molecular psychiatry.* 2014;19(6):659-667.
13. Bölte S, Poustka F, Constantino JN. Assessing autistic traits: cross-cultural validation of the social responsiveness scale (SRS). *Autism Research.* 2008;1(6):354-363.
14. McConachie H, Parr JR, Glod M, et al. Systematic review of tools to measure outcomes for young children with autism spectrum disorder. *Health Technology Assessment.* 2015;19(41):1-506.
15. Ho DE, Imai K, King G, Stuart EA. MatchIt: nonparametric preprocessing for parametric causal inference. *Journal of Statistical Software.* 2011;42(8):1-28.
16. Diamond A, Sekhon JS. Genetic matching for estimating causal effects: A general multivariate matching method for achieving balance in observational studies. *Review of Economics and Statistics.* 2013;95(3):932-945.
17. Zou H, Hastie T. Regularization and variable selection via the elastic net. *Journal of the Royal Statistical Society: Series B (Statistical Methodology).* 2005;67(2):301-320.
18. Hendricks P, Ahn W-Y. Easyml: Easily Build And Evaluate Machine Learning Models. *bioRxiv.* 2017:137240.
19. Vilares I, Wesley MJ, Ahn W-Y, et al. Predicting the knowledge–recklessness distinction in the human brain. *Proceedings of the National Academy of Sciences.* 2017;114(12):3222-3227.
20. Team RC. R: A language and environment for statistical computing. R Foundation for Statistical Computing, Vienna, Austria. 2013. 2014.
21. Ho D, Imai K, King G. Stuart Ea (2011). MatchIt: nonparametric preprocessing for parametric causal inference. *J Stat Soft.*42:1-28.

22. McArtor DB, Lubke GH, Bergeman CS. Extending multivariate distance matrix regression with an effect size measure and the asymptotic null distribution of the test statistic. *Psychometrika.* 2016.
23. Anderson JS, Nielsen JA, Froehlich AL, et al. Functional connectivity magnetic resonance imaging classification of autism. *Brain : a journal of neurology.* 2011;134(Pt 12):3742-3754.
24. Menon V. Salience Network. *In: Arthur W. Toga, editor. Brain Mapping: An Encyclopedic Reference, vol. 2, pp. 597-611. Academic Press: Elsevier.*2015:597-611.
25. Mak LE, Minuzzi L, MacQueen G, Hall G, Kennedy SH, Milev R. The Default Mode Network in Healthy Individuals: A Systematic Review and Meta-Analysis. *Brain Connectivity.* 2017.
26. Katuwal GJ, Baum SA, Cahill ND, Michael AM. Divide and Conquer: Sub-Grouping of ASD Improves ASD Detection Based on Brain Morphometry. *Plos One.* 2016;11(4):e0153331.
27. Pua EPK, Malpas CB, Bowden SC, Seal ML. Different brain networks underlying intelligence in autism spectrum disorders. *Human Brain Mapping.* 2018;39(8):3253-3262.
28. Dawson G, Webb S, Schellenberg GD, et al. Defining the broader phenotype of autism: genetic, brain, and behavioral perspectives. *Development & Psychopathology.* 2002;14(3):581-611.
29. Bishop DVM, Maybery M, Wong D, Maley A, Hallmayer J. Characteristics of the broader phenotype in autism: A study of siblings using the children's communication checklist-2. *American Journal of Medical Genetics Part B: Neuropsychiatric Genetics.* 2006;141B(2):117-122.
30. Mensen VT, Wierenga LM, van Dijk S, et al. Development of cortical thickness and surface area in autism spectrum disorder. *NeuroImage: Clinical.* 2017;13:215-222.
31. Fornito A, Bullmore ET, Zalesky A. Opportunities and Challenges for Psychiatry in the Connectomic Era. *Biological Psychiatry: Cognitive Neuroscience and Neuroimaging.* 2017;2(1):9-19.
32. Grayson DS, Fair DA. Development of large-scale functional networks from birth to adulthood: a guide to neuroimaging literature. *NeuroImage.* 2017;160:15-31.

Tables

Table 1. Descriptive statistics of matched samples

Group	n	Sex	Age	IQ	SRS
ASD	100	n=84 males	11.43 (3.55)	110.58 (13.18)	91.7 (28.42); Range: 11 - 162
Controls	100	n=84 males	11.43 (3.55)	110.70 (13.18)	19.7 (13.0); Range: 1-57

Note. SRS: Social Responsiveness Scale. Higher score indicates more severe ASD symptoms.

Figure Legends

Figure 1. Subject-level distance-based pipeline. **A:** Each ASD case was individually matched to one control participant in age, sex, IQ and acquisition site. **B:** For every matched pair, within-pair Euclidean distances (Δ) on symptom severity variables and morphometry of brain region-of-interests (ROI) were computed. **C:** Using a machine learning approach, regularized regression with elastic net penalization was implemented to test the association between within-pair ΔROI and Δsymptom severity. A subset of the sample (33%) was held out as an independent out-of-sample test set. Remaining data was used as a training set to obtain cross-validated model weights for feature selection. The trained coefficient weights were then used to generate predictions and model fit parameters in the held-out test set. **D:** Finally, out-of-sample model fits were evaluated against a null distribution of 5,000 permutations.

Figure 2. Individual intrapair differences for cortical thickness (A) and surface area (B). *Rows are cortical features, columns are matched subject pairs. Each row represents intrapair distance data for a specific cortical region across all subjects. Each column represents intrapair distance data for a specific subject pair across all cortical regions. Brighter heatmap gradient (yellow) indicates higher intrapair distance.*

Figure 3. Individual differences in brain regions underlying subject-level symptom severity variation in ASD. Color bars represent mean beta coefficients of selected cortical features from the machine-learning trained regularized regression model. **A:** Cortical thickness features associated with symptom severity variation in ASD **B:** Surface area features associated with symptom severity variation in ASD. ***Note.*** *CAC: caudal anterior cingulate gyrus; CUN: cuneus; ENT: entorhinal; FUS: fusiform gyrus; INFP: inferior parietal gyrus; INS: insula; ISTC: isthmus cingulate gyrus; IT: inferior temporal gyrus; LH: left hemisphere; LIN: lingual gyrus; MORB: medial orbitofrontal; MT: middle temporal gyrus; PCAL: pericalcerine; PC: posterior cingulate gyrus; PORS: pars orbitalis; RH: Right hemisphere; PTRI: pars triangularis; RMF: rostral middle frontal gyrus.*

Figure 1. Subject-level distance-based pipeline.

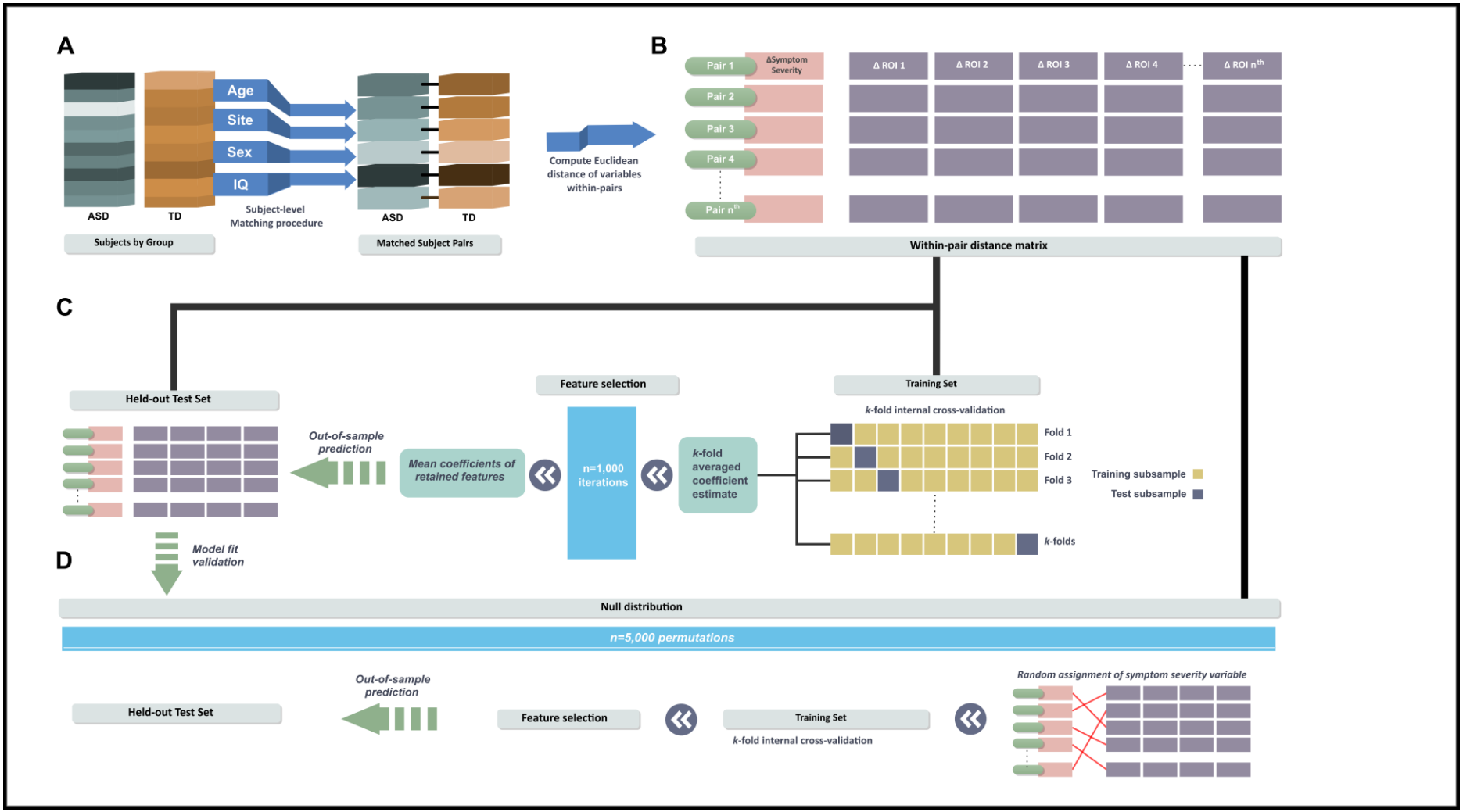

Figure 2. Individual intrapair differences for cortical thickness (A) and surface area (B).

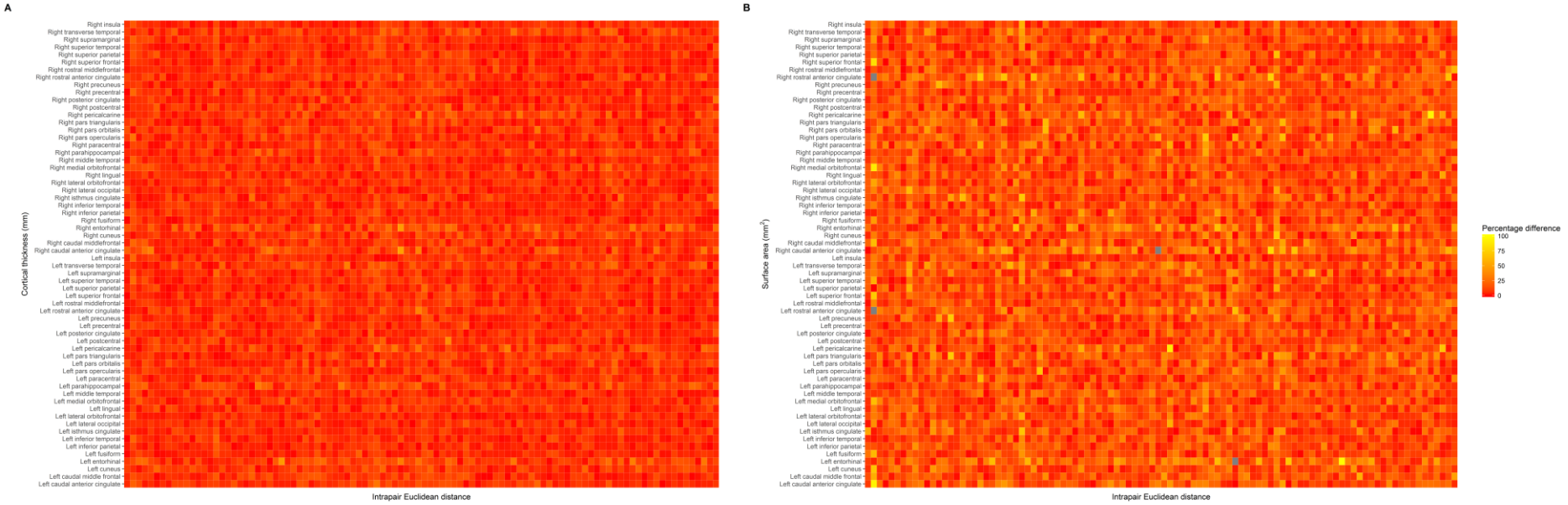

Figure 3. Individual differences in brain regions underlying subject-level symptom severity variation in ASD.